Molecular Biology of the Cell
Vol. 16, 4423–4436, September 2005

Taxol-stabilized Microtubules Can Position the Cytokinetic Furrow in Mammalian Cells[V]

Katie B. Shannon,* Julie C. Canman,† C. Ben Moree,* Jennifer S. Tirnauer,‡ and E. D. Salmon*

*Department of Biology, University of North Carolina, Chapel Hill, NC 27599-3280; †Institute of Molecular Biology, University of Oregon, Eugene, OR 97403; and ‡Center for Molecular Medicine, University of Connecticut Health Center, Farmington, CT 06030-3101

Submitted November 8, 2004; Revised June 3, 2005; Accepted June 14, 2005
Monitoring Editor: Thomas Pollard

How microtubules act to position the plane of cell division during cytokinesis is a topic of much debate. Recently, we showed that a subpopulation of stable microtubules extends past chromosomes and interacts with the cell cortex at the site of furrowing, suggesting that these stabilized microtubules may stimulate contractility. To test the hypothesis that stable microtubules can position furrows, we used taxol to rapidly suppress microtubule dynamics during various stages of mitosis in PtK1 cells. Cells with stabilized prometaphase or metaphase microtubule arrays were able to initiate furrowing when induced into anaphase by inhibition of the spindle checkpoint. In these cells, few microtubules contacted the cortex. Furrows formed later than usual, were often aberrant, and did not progress to completion. Images showed that furrowing correlated with the presence of one or a few stable spindle microtubule plus ends at the cortex. Actin, myosin II, and anillin were all concentrated in these furrows, demonstrating that components of the contractile ring can be localized by stable microtubules. Inner centromere protein (INCENP) was not found in these ingressions, confirming that INCENP is dispensable for furrow positioning. Taxol-stabilization of the numerous microtubule–cortex interactions after anaphase onset delayed furrow initiation but did not perturb furrow positioning. We conclude that taxol-stabilized microtubules can act to position the furrow and that loss of microtubule dynamics delays the timing of furrow onset and prevents completion. We discuss our findings relative to models for cleavage stimulation.

INTRODUCTION

Cytokinesis results in the physical separation of daughter cells, which is accomplished by contractile forces generated by actin and myosin II (Schroeder, 1972; Mabuchi and Okuno, 1977). Cytokinesis normally occurs at the spindle equator during anaphase, after chromosome segregation. It is essential that cytokinesis be spatially and temporally regulated to ensure correct partitioning of genetic material and to prevent polyploidy. In animal cells, the position of the mitotic spindle establishes the plane of the cleavage furrow, because repositioning the spindle during mitosis by centrifugation or micromanipulation leads to a relocation of the furrow (Conklin, 1917; Harvey, 1935; Rappaport and Ebstein, 1965; Rappaport and Rappaport, 1974). Disrupting or removing the spindle from sea urchin eggs before the beginning of anaphase completely blocks furrow formation, whereas the spindle is not required for furrowing after anaphase (Beams and Evans, 1940; Hiramoto, 1956; Hamaguchi, 1975). Therefore, furrow positioning occurs during a small window in the cell cycle during early anaphase.

This article was published online ahead of print in *MBC in Press* (http://www.molbiolcell.org/cgi/doi/10.1091/mbc.E04–11–0974) on June 22, 2005.

[V] The online version of this article contains supplemental material at *MBC Online* (http://www.molbiolcell.org).

Address correspondence to: Katie B. Shannon (ktphd@email.unc.edu).

The components of the spindle required for furrow positioning have been extensively investigated, and, surprisingly, many parts of the spindle are not essential for the initiation of cytokinesis. Microtubules are both necessary and sufficient for furrow positioning, because cells containing only asters or only the central spindle were able to induce furrowing (Alsop and Zhang, 2003), whereas cells lacking microtubules fail to do so (Hamaguchi, 1975; Canman *et al*., 2000). Although microtubules are indispensable for furrow initiation, the nature of the signal and the population of microtubules responsible continue to be debated. Experiments in echinoderm embryos led to a model that asters stimulate furrow formation at the equator, where signals from overlapping microtubules are maximal (Rappaport, 1986). Observations in mammalian cells suggest that the central spindle, not astral, microtubules positively regulate furrow formation (Cao and Wang, 1996). A model proposing negative regulation of furrowing by microtubules, based on experiments in *Caenorhabditis elegans*, speculates that the formation of the central spindle may result in furrowing due to removal of microtubule inhibition of furrowing at the equator (Dechant and Glotzer, 2003).

These models all propose a role for overlapping microtubule plus ends either at the equator or the central spindle to produce the signal for furrow formation. Recently, the requirement for a bipolar spindle for cytokinesis was tested in animal cells using the small molecule inhibitor monastrol (Canman *et al*., 2003). This study showed that cells with monopolar spindles can undergo cytokinesis, with the furrow forming on the side of the cell facing the chromosomes rather than the pole. Polar microtubules were found to be

dynamic, whereas a subset of microtubules extending past chromosomes formed stable interactions with the cell cortex at the site of furrowing (Canman *et al*., 2003). This led to a model in which microtubule dynamics contribute to furrow positioning, with a subpopulation of relatively stable microtubules interacting with the equatorial cortex to promote furrow formation, and dynamic microtubules at the polar regions helping to suppress ectopic furrowing (Canman *et al*., 2003). Therefore, microtubule dynamics, rather than their location at asters or the central spindle, may be important for furrow positioning.

Taxol is commonly used to perturb microtubule dynamics, because it has been shown to stabilize microtubules and to promote microtubule assembly in vitro and in vivo (Schiff *et al*., 1979; Schiff and Horwitz, 1980; De Brabander *et al*., 1981, 1986). Previous studies on cytokinesis using taxol produced conflicting results: furrow initiation in sea urchin eggs was blocked, but in sand dollar eggs it was not (Salmon and Wolniak, 1990; Hamaguchi, 1998). Addition of taxol to PtK1 cells before the metaphase–anaphase transition results in a mitotic block (De Brabander *et al*., 1986).

PtK1 cells treated with taxol after anaphase onset showed either a reduced degree and rate of furrowing (Snyder and Mullins, 1993; Snyder and McLelland, 1996) or no effect on the timing of cytokinesis (Amin-Hanjani and Wadsworth, 1991). These PtK1 studies were not able to address furrow positioning, because taxol treatment occurred after the small window in early anaphase when furrow position is established.

To test the hypothesis that stable microtubules can position furrows, we imaged cytokinesis in cells in which microtubules were stabilized by taxol. Unlike previous experiments, cells were treated with taxol before anaphase and then induced into anaphase by inhibiting the spindle checkpoint. We found that taxol-stabilized microtubules are sufficient for furrow initiation and that the position of furrowing correlates with the interaction of a stable spindle microtubule with the cell cortex. Our data also confirm that although dynamic microtubules are not necessary for furrow initiation, they are required for the normal timing of furrow initiation and the completion of cytokinesis.

MATERIALS AND METHODS

Cell Culture and Transfection

PtK1 cells (American Type Culture Collection, Manassas, VA) were grown on coverslips and maintained in Ham's F-12 medium, pH 7.2 (Sigma, St. Louis, MO) supplemented with 10% fetal bovine serum, 100 U/ml penicillin, 0.1 mg/ml streptomycin, and 0.25 μg/ml amphotericin B in a 37°C, 5% CO_2 incubator. Human EB1 was cloned into the *Xho*I-BamH1 restriction sites of pEGFP-N1 (BD Biosciences Clontech, Palo Alto, CA) and transfected into PtK1 cells using the Effectene reagent (QIAGEN, Valencia, CA) according to the manufacturer's instructions. Cells were selected for EB1 expression using 200 μg/ml G418. Only cells expressing a low level of EB1, which did not bundle microtubules or block microtubule dynamics were analyzed. For microinjection or imaging experiments, cells were incubated in phenol red-free L-15 medium, pH 7.2 (Sigma), supplemented as described for Ham's F-12 with addition of 0.3 U/ml Oxyrase (Oxyrase, Mansfield, OH) per milliliter of media to minimize photobleaching. Taxol was added to media from a stock solution of 10 mM in dimethyl sulfoxide for a final concentration of 10 μM.

Immunofluorescence

Cells were lysed in freshly prepared 0.5% Triton X-100 in PHEM buffer (60 mM PIPES, 25 mM HEPES, 10 mM EGTA, and 4 mM $MgSO_4$, pH 6.9) at 37°C and fixed in freshly prepared 4% formaldehyde in PHEM buffer at 37°C for 20 min. Cells were then rinsed three times for 5 min in phosphate-buffered saline with 0.05% Tween 20 (PBST) and blocked overnight at 4°C in PHEM with 5% donkey serum (except for PRC1 and tubulin immunofluorescence, for which cells were first fixed, then rinsed, and then lysed before blocking). Primary antibodies were diluted into PHEM with 5% donkey serum and cells were incubated at room temperature for an hour. After three 5-min PBST washes, X-rhodamine-labeled secondary donkey anti-rabbit (Jackson ImmunoResearch Laboratories, West Grove, PA) and/or Alexa 488-labeled phalloidin (Molecular Probes, Eugene, OR) diluted 1:100 in PHEM with 5% donkey serum were added for 45 min.

Rabbit anti-anillin antibody was a generous gift from Christine Field (Harvard Medical School, Boston, MA) and was used at 1:600. Rabbit anti-inner centromere protein (INCENP) antibody was kindly provided by Aaron Straight (Stanford University School of Medicine, Stanford, CA) and used at 1:1500. Antibody to PRC1 (H-170) (Santa Cruz Biotechnology, Santa Cruz, CA) was used at 1:500, and anti-tubulin antibody DM1A (Sigma) at 1:300. The rabbit polyclonal antibody to nonmuscle myosin II was purchased from Biomedical Technologies (Cambridge, MA) and used for immunofluorescence as per manufacturer's instructions.

Microinjection

Before microinjection, coverslips were mounted in modified Rose chambers (Rieder and Hard, 1990) lacking the top coverslip, and chambers were filled with L-15 media. A circle was inscribed on the bottom coverslip using a diamond-tip scribing objective (Carl Zeiss, Thornwood, NY) and was used as a reference to relocate injected cells. Injections were performed on a Zeiss IM microscope equipped with phase contrast optics and a 40×/0.75 numerical aperture (NA) objective. The microinjection system is essentially as described previously (Waters *et al*., 1996). His-Mad2ΔC was purified as described previously (Canman *et al*., 2002) and injected at a needle concentration of 5 mg/ml in human embryonic kidney (HEK) (20 mM HEPES, 100 mM KCl, and 1 mM dithiothreitol, pH 7.7). Cells were treated with 10 μM taxol for a minimum of 30 min before microinjection of Mad2ΔC. The X-rhodamine-labeled tubulin was prepared as described previously (Hyman *et al*., 1991; Waterman-Storer *et al*., 1998), or rhodamine-labeled tubulin was purchased from Cytoskeleton (Denver, CO) and injected at a needle concentration of 1 mg/ml. For time-lapse microscopy on the injection scope, the top of the chamber was sealed using mineral oil. Chambers used for imaging on the confocal microscope were sealed using a top coverslip and filled with fresh, dye-free high glucose L-15 medium supplemented with 0.3 U/ml oxygen-scavenging system Oxyrase (Oxyrase).

Microscopy and Image Acquisition

Images of immunofluorescently labeled cells were obtained with a Hamamatsu ER cooled charge-coupled device (CCD) digital camera (Hamamatsu Photonics, Bridgewater, NJ), using a Nikon TE 300 inverted microscope equipped with a 100×/1.4 NA Plan Apo Phase 3 objective lens, a 100-W mercury arc fluorescence light source, and a Sutter filter wheel. Digital images were acquired by MetaMorph image processing software (Universal Imaging, Downingtown, PA). Z series optical sections through each cell were obtained at 0.2-μm steps, using MetaMorph software to control the stepping motor on the Nikon TE 300.

For live cell imaging, cells were imaged using the spinning disk confocal microscope essentially as described previously (Maddox *et al*., 2003). Briefly, images were obtained on a Nikon TE300 inverted microscope equipped with an OrcaER cooled CCD camera (Hamamatsu Photonics). Pairs of fluorescence and phase contrast images were obtained using a 100× 1.4 NA Plan Apo Phase 3 objective with excitation light supplied from an optical fiber connected to a 100-W argon-krypton air-cooled laser. The microscope and shutters were controlled by MetaMorph imaging software, using a Nikon stepping motor to take 0.5-μm steps in the *z*-axis. Stage temperature was maintained at ~37°C using an ASI 400 air curtain incubator (Nevtek, Burnsville, VA).

Data Analysis

Image deconvolution of stacks of optical sections was performed with a DeltaVision deconvolution system and Softworx software (Applied Precision, Issaquah, WA). For cell area calculations, the region tool in MetaMorph was used to trace the cell boundary at the time of anaphase onset in phase contrast images, and the area was calculated using calibrated region measurements. All averages, standard deviations, and p values were calculated using Excel (Microsoft, Redmond, WA).

RESULTS

Taxol Rapidly Suppresses Microtubule Plus End Dynamics

We used taxol to suppress microtubule dynamics in living PtK1 cells. Taxol binds to β tubulin in the microtubule lattice, causing stabilization under conditions that normally result in depolymerization: when the GTP-binding site contains GDP or microtubules are exposed to cold or calcium (Schiff *et al*., 1979; Salmon and Wolniak, 1984; Amos and Lowe, 1999). Taxol has been shown to suppress the dynam-

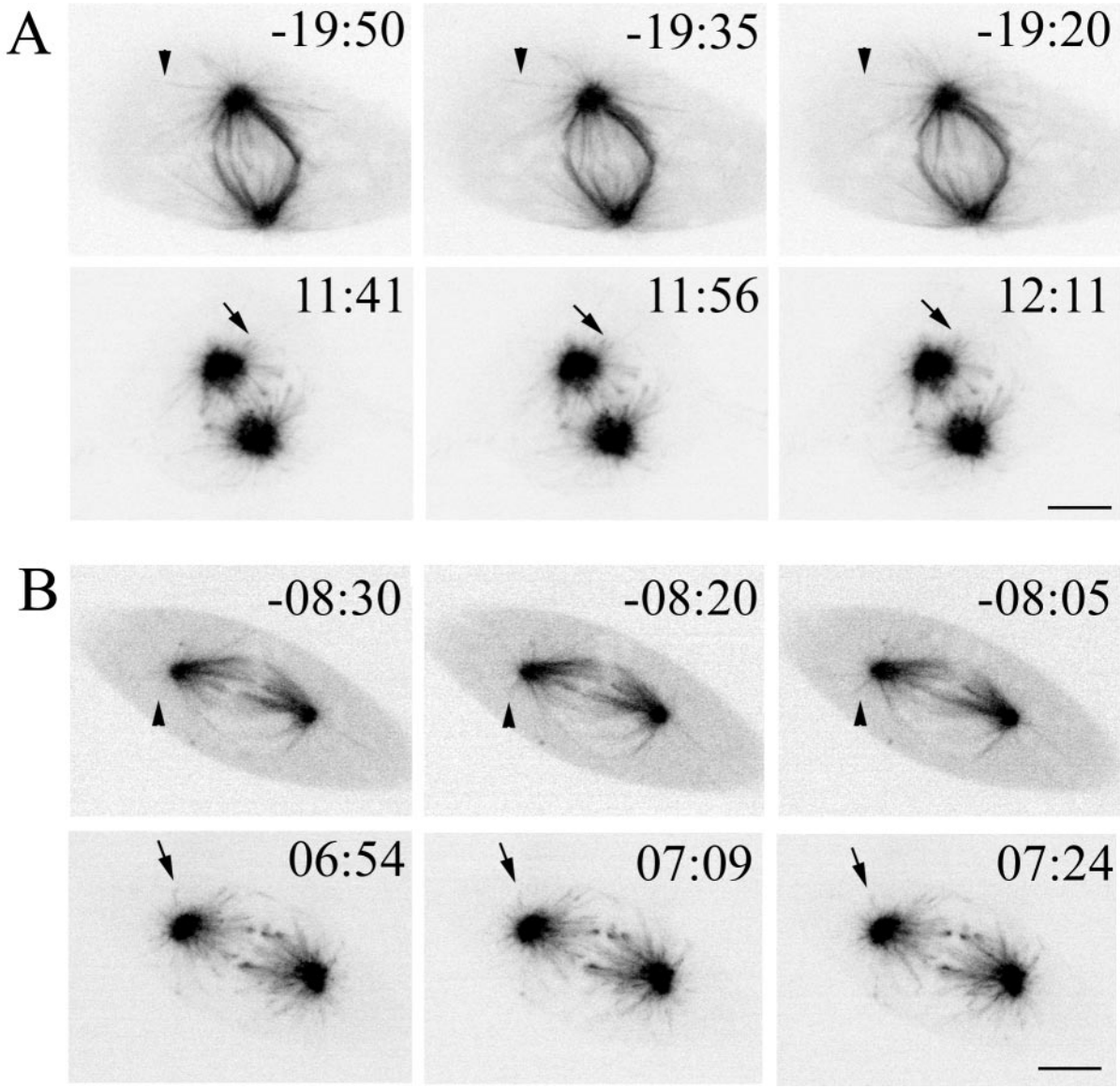

Figure 1. Addition of taxol stabilizes microtubules and suppresses dynamics of individual microtubules in living PtK1 cells. (A and B) Two cells are shown before (top) and after (bottom) addition of 10 μM taxol at T = 00:00. Arrowheads are fixed and provide a reference point for the growth and shrinkage of nearby microtubules in untreated cells. Arrows show stable astral microtubules after taxol addition. Contrast was enhanced for visualization of astral microtubules. Time is in minutes:seconds. Bar, 5 μm.

ics of individual microtubules in living human cells (Yvon *et al*., 1999). We confirmed by live cell imaging of green fluorescent protein (GFP)-α tubulin-expressing PtK2 cells (Rusan *et al*., 2001) that a dose of 10 μM taxol results in a suppression of microtubule dynamics during mitosis (Figure 1). Within minutes of addition, taxol induced characteristic changes to the spindle. These included the formation of many short astral microtubules, shortening of the spindle, and polymerization of some short microtubules not associated with the spindle (Figure 1) (De Brabander *et al*., 1981; Snyder and Mullins, 1993). After these initial changes, the spindle structure was "frozen," because the loss of microtubule dynamics prevents further spindle reorganization.

To determine how quickly taxol suppressed microtubule dynamics, we used PtK1 cells expressing EB1-GFP. Normally, EB1 associates strongly with growing, but not stable, plus ends (Morrison *et al*., 1998; Tirnauer *et al*., 2002). We observed live EB1-GFP-expressing mitotic cells before and after treatment with 10 μM taxol using spinning disk confocal microscopy. Analysis of these cells showed that EB1 was lost from the plus ends of microtubules within an average of 5 min 35 s $\pm$ 48 s after taxol addition (n = 7), as shown in Figure 2, A–C. After strong EB1-GFP association with microtubule plus ends was lost, the weak association of EB1 with the microtubule lattice and spindle poles persisted (Figure 2C) (Tirnauer *et al*., 2002). This shows that taxol rapidly suppresses microtubule dynamics in live PtK1 cells.

Because EB1 is lost from plus ends of microtubules stabilized by taxol, we were interested in determining whether the stable microtubules normally seen during anaphase at the equatorial cortex exhibited EB1 localization. Rhodamine-labeled tubulin was microinjected into EB1-GFP-expressing mitotic cells, and these cells were visualized during anaphase using spinning disk confocal microscopy. EB1 ini-

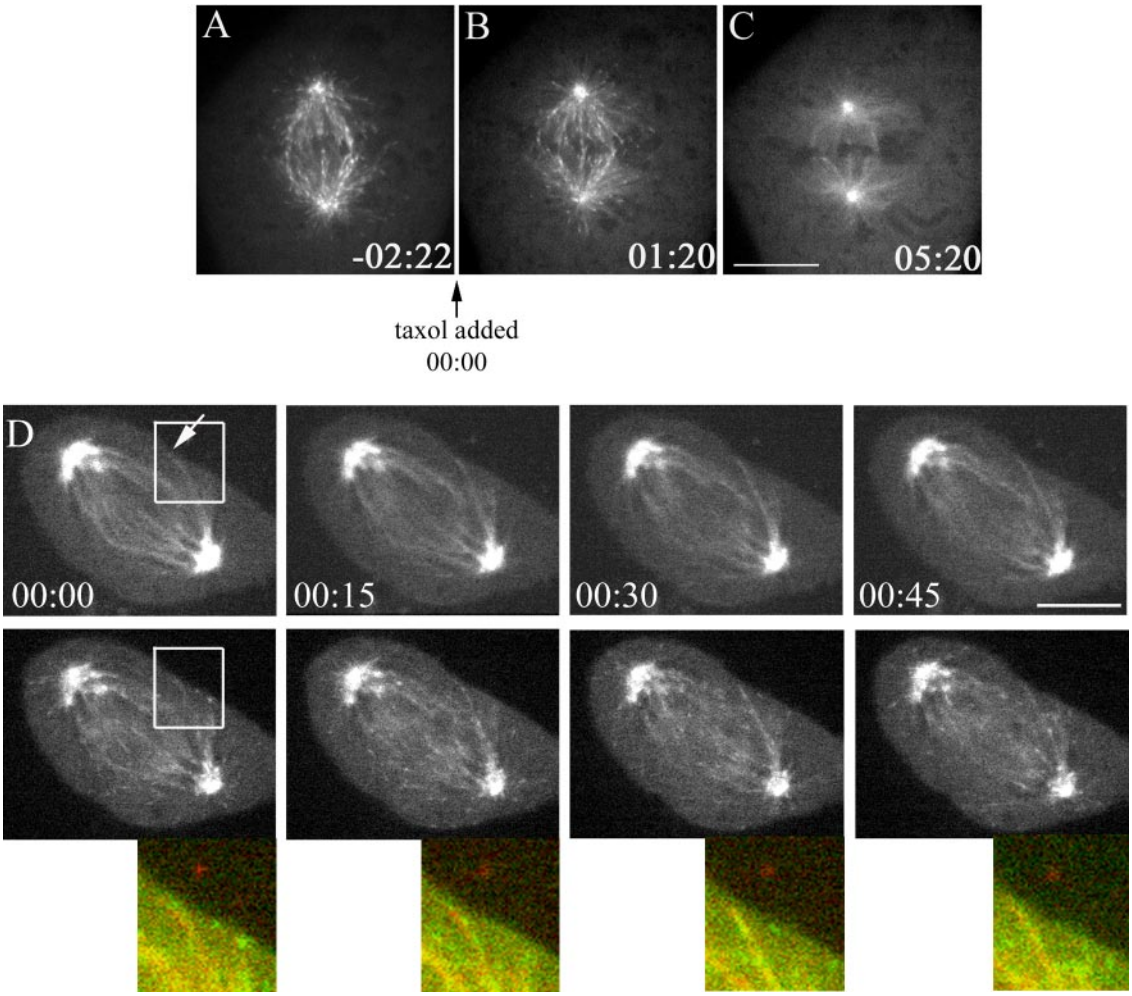

Figure 2. Stable microtubules lose EB1 tip localization. (A) EB1-GFP localization to growing microtubule plus ends before addition of taxol. 10 μM taxol was added at T = 00:00. (B) Localization of EB1-GFP 1 min 20 s after taxol addition shows that microtubule polymerization is still occurring. (C) EB1-GFP 5 min 20 s after taxol addition. EB1 is no longer localized to microtubule ends, but it is seen diffusely along the microtubule lattice and at spindle poles. (D) Untreated EB1-GFP cell injected with rhodamine-labeled tubulin. T = 00:00 was assigned to first image shown. Top, tubulin fluorescence. Arrow indicates a stable microtubule–cortex interaction. Middle, EB1-GFP. White box indicates region shown in bottom panel. Bottom, 2× magnification of combined tubulin (red) and EB1-GFP (green) fluorescence. Time is in minutes:seconds. Bar, 10 μm.

tially localized to the plus ends of microtubules that grew out to the equatorial cortex. However, this EB1 signal did not persist after stable association of a microtubule with the cortex. Figure 2D shows a microtubule with EB1-GFP at the tip reaching the cortex (00:00), but the bright EB1 signal is lost, whereas the microtubule remains in contact with the cortex. A low level of EB1 can be seen along the lattice (Figure 2D), similar to EB1 localization in the presence of taxol. No accumulation of EB1-GFP in the furrow was evident (our unpublished data). These data indicate that microtubule growth is substantially suppressed at the ends of stable microtubules in contact with the cortex.

Stabilization of Microtubules before Anaphase Onset Disrupts Cytokinetic Furrow Position, Timing, and Completion

We first examined the effects of microtubule stabilization before the window of furrow formation during early anaphase. Because treatment of mitotic PtK1 cells with taxol before the metaphase–anaphase transition results in a mitotic arrest, we used a dominant negative-truncated Mad2 His fusion protein, Mad2ΔC, to bypass this mitotic arrest (Canman *et al*., 2002). Mad2ΔC has been shown to induce premature anaphase onset in prometaphase cells without affecting the timing or morphology of the subsequent cytokinesis (Canman *et al*., 2002). Taxol treatment coupled with the use of Mad2ΔC to induce anaphase allowed us to ask whether cells in which all microtubules are stabilized can initiate furrows. Cells arrested in prometaphase or metaphase by taxol treatment were injected with Mad2ΔC and followed by time-lapse microscopy. Mad2ΔC induced anaphase onset (visualized by separation of sister chromatid arms) in taxol-treated cells after an average of 17 ± 8 min after injection (n = 14), similar to control cells (Table 1). Also similar to control cells, taxol-treated, Mad2ΔC-injected cells spent an average of 58 ± 24 min in the cytokinesis phase (C phase) before respreading and reforming the nuclear envelope. This 1-h window after anaphase onset in which cells are capable of furrowing is similar to previous observations

Table 1. Comparison of furrow formation in control and taxol-treated cells

	n	Avg time from injection to anaphase	Avg time from anaphase onset to furrow[a]	Avg time in C phase	No furrow	Furrow	Abnormal furrow
Untreated	5	14:12 ± 5:03	11:21 ± 4:25	42:30 ± 10:26	0	5	0
Taxol	14	17:25 ± 7:58	30:01 ± 15:18	57:40 ± 24:25	5	9	6

The time from injection to anaphase onset, anaphase onset to furrow formation, and average time in C phase was measured by time-lapse microscopy. Time is in minutes:seconds and expressed as mean ± SD. Control cells (untreated, n = 5 cells) were injected in prometaphase with Mad2ΔC. Taxol-treated cells (taxol, n = 14 cells) arrested in prometaphase or metaphase were injected with Mad2ΔC. The number of cells forming no furrow, a normal furrow, or furrows abnormal in position or number is shown.

[a] $p < 0.01$.

(Martineau *et al*., 1995; Canman *et al*., 2000; Shannon *et al*., 2002; Straight *et al*., 2003).

We saw three phenotypes in cells entering anaphase with taxol-stabilized microtubules: no furrowing, normal furrowing, and abnormal furrowing (Figure 3 and Table 1). In none of these cases did cytokinesis progress to completion. Of the 14 cells assayed, five did not form any cleavage furrows before respreading and exiting C phase (Figure 3A, Figure 3A Movie, and Table 1). Three cells initiated normal furrows, which began as two ingressions near the equator perpendicular to the spindle axis (Figure 3B and Figure 3B Movie). Six cells furrowed abnormally, having either an incorrect number or location of furrows (Table 1). Two cells had three ingressions, two cells had only a one-sided furrow, and two cells furrowed on an axis not perpendicular to the spindle. An example of a cell that furrowed on an abnormal axis is shown in Figure 3C (Figure 3C Movie available online).

In the nine cells that formed furrows, either normal or abnormal, the time from anaphase onset to furrow induction was longer than controls, 30 ± 15 min versus 11 ± 4 min ($p < 0.01$) (Table 1). Therefore, taxol stabilization of micro-

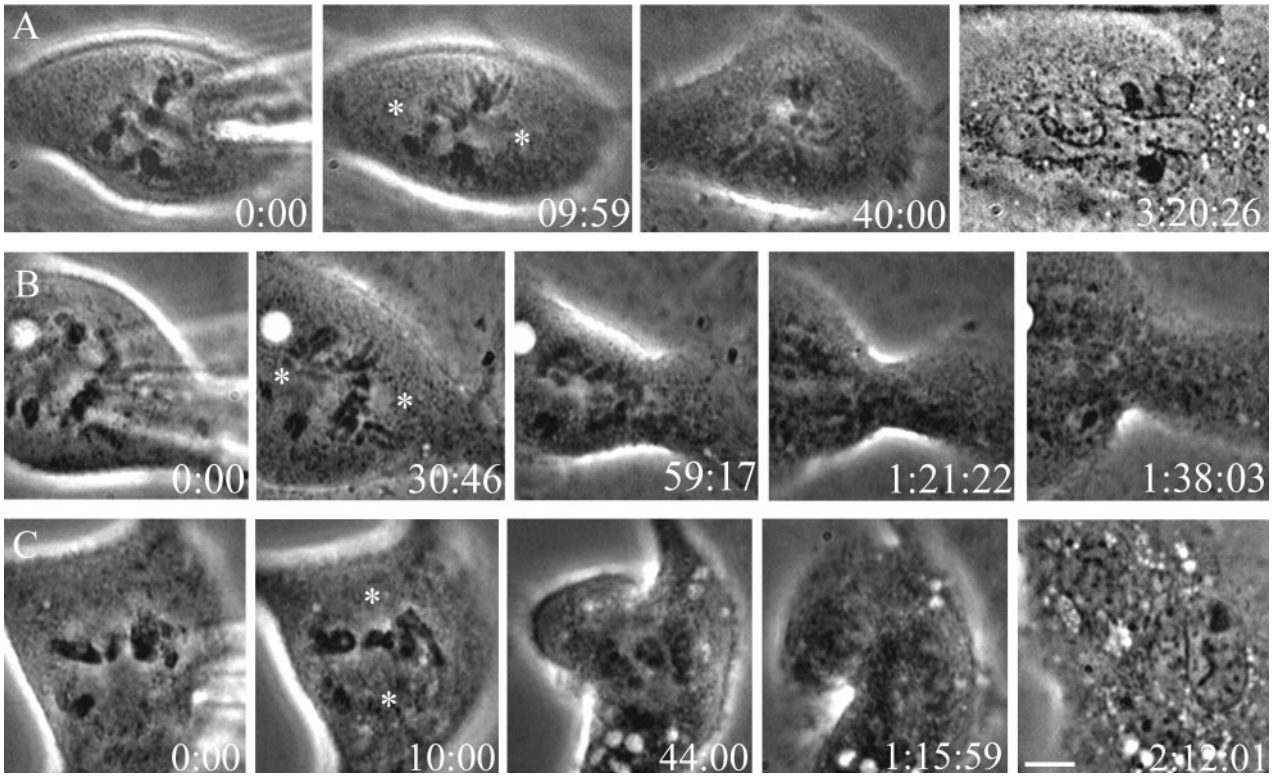

Figure 3. Stabilization of microtubules before anaphase onset produces three phenotypes. Cells in 10 μM taxol were injected with Mad2ΔC at T = 00:00. Asterisks indicate approximate position of spindle poles. (A) No furrow formation. After injection, the cell entered anaphase (T = 9:59) and did not furrow before respreading and entering interphase (T = 3:20:26). (B) Normal furrow positioning. The cell entered anaphase (T = 30:46) and furrowed with two ingressions, which formed perpendicular to the spindle axis. Furrows were maximally ingressed at T = 1:21:22, and one furrow regressed as the cell entered interphase (T = 1:38:03). (C) Abnormal furrow positioning. The cell formed two ingressions (T = 44:00), but the furrow did not form on a plane bisecting the spindle, because one furrow was initiated near the pole (top asterisk). Both furrows eventually regressed (T = 1:15:59) as the cell entered interphase (T = 2:12:01). Time is shown in hours:minutes: seconds. Bar, 5 μm.

tubules delayed, but did not prevent, the onset of furrowing in these cells. In all cases, cells failed to complete cytokinesis. Furrowing often did not progress to the midpoint of the cell, and most furrows regressed around the end of C phase.

Random cortical contractions occur during C phase in cells treated with nocodazole to depolymerize microtubules and induced to enter anaphase by microinjection of Mad2ΔC (Canman *et al*., 2000). We saw no evidence for these random cortical ingressions in the taxol-treated cells induced into anaphase. This was true both for cells that exhibited furrowing and cells that did not furrow. This indicates that the presence of microtubule polymer, rather than dynamics, is important to suppress global contractility.

We looked for differences between cells that furrowed and those that did not. Cell cycle state did not seem to differentiate the two populations, because cells with a metaphase plate were not more likely to furrow or position furrows normally than cells with stabilized prometaphase spindles. Formation of a midzone microtubule complex is prevented in cells treated with taxol before anaphase onset, but this disruption did not differ between cells that did or did not exhibit furrowing (see below). Cell area did seem to be an important variable, because cells with a larger area were less likely to furrow than cells with smaller areas. Area measurements at anaphase onset showed that the average area of cells that failed to form furrows was 915 μm^2, whereas those that did form furrows had an average area of 603 μm^2 ($p < 0.05$). Therefore, cells that failed to furrow were 50% larger in area on average than those that did produce furrows.

From these observations, we conclude that PtK1 cells induced to enter anaphase after microtubule stabilization are capable of initiating furrows, although these furrows often have an abnormal number of ingressions or are mispositioned relative to the spindle. These data suggest that dynamic microtubule plus ends are not required for furrow induction or for suppression of the random cortical contractions that occur during anaphase in the absence of microtubules. However, the failure of some cells to initiate furrows, as well as the high frequency of abnormal furrows and the delay in furrow initiation, suggest that microtubule organization, density, or dynamics is key for some aspect(s) of furrow positioning or signaling, as well as completion of cytokinesis.

Stable Microtubule Plus Ends Contact the Cell Cortex at the Site of Furrowing

We suspected that one reason cells with smaller area might be more likely to initiate furrows is that they were biased toward increased incidence of microtubule–cortex interactions. Because furrows have been shown to be associated with stable microtubules (Canman *et al*., 2003), we imaged microtubules in taxol-treated cells to determine whether stable microtubules contacted the cell cortex before the initiation of furrowing. To do this, we imaged cells that were microinjected with rhodamine-labeled tubulin and Mad2ΔC and subsequently treated with 10 μM taxol. When cells with taxol-stabilized spindles were induced into anaphase, they retained the short astral microtubules typical of preanaphase spindles. Microtubule arrays were examined using image deconvolution and single plane projections of multiple Z sections acquired by spinning disk confocal microscopy. As in the previous experiment, pleiotropic effects on furrowing were observed: of twelve cells analyzed, three furrowed normally, six abnormally, and three did not furrow. In all cases, the presence or absence of microtubule–cortex interactions correlated with furrowing. The nine cells that furrowed produced a total of seventeen ingressions, all of which exhibited a microtubule–cortical interaction at the site before furrow initiation. Four of the six cells that furrowed abnormally exhibited furrowing in a polar region of the cell. These cells had seven polar furrows total, each of which was preceded by a polar astral microtubule interacting with the polar cortex. The three cells that did not furrow lacked any contacts between spindle microtubules and the cell cortex (see below).

Figure 4 shows the relationship between microtubules and furrowing in a control cell, a cell that did not furrow, a cell that furrowed near the equator, and a cell that furrowed abnormally near the pole. Figure 4A (Figure 4A Movie available online) shows a control cell injected with rhodamine-labeled tubulin and Mad2ΔC. During anaphase, numerous microtubules extended from the spindle poles to the peripheral equatorial cortex (arrows). The furrow formed ≈10 min after this image was acquired, in the region of the multiple contacts between the microtubules and the cortex (Figure 4A′ and Figure 4A′ Movie). An example of a taxol-treated cell that did not furrow is shown in Figure 4, B and B′. No spindle microtubule plus ends contacted the cell periphery (Figure 4B and Figure 4B Movie), and the cell failed to form a cleavage furrow (Figure 4B′ and Figure 4B′ Movie) before exiting mitosis. Note the large area of the cell compared with other cells in the figure and lack of random cortical contractions. We are confident that we did not miss a stable microtubule in any of the cells that failed to furrow, because Z sections covered the entire height of the cells. An example of a stable microtubule interacting with the cortex near the equator at the eventual site of furrow formation in a taxol-treated cell is shown in Figure 4, C–C″. The single plane projection of deconvolved Z series images shows microtubule(s) extending out from the spindle to the cell periphery near the equator (Figure 4C, arrow). Single plane images reveal the interaction of the microtubule(s) with the cortex (arrow) before furrow initiation (Figure 4C′ and Figure 4C′ Movie). The furrow begins at the site of microtubule contact and ingresses about halfway through the cell before regressing (Figure 4C″ and Figure 4C″ Movie). Notice that the top of the cell, which lacks microtubule interactions, does not furrow. Figure 4, D–D″, is an example of a cell with an abnormally positioned furrow in the polar region of the cell. Figure 4D shows the single plane projections of deconvolved Z series images showing all the microtubules in the cell at two time points, indicating that there is no spindle reorganization during the time course of these experiments due to the lack of microtubule dynamics. The arrow points to a microtubule extending from the spindle pole to the polar cortex before the induction of the furrow. Single plane images in Figure 4, D′ and D″ (Figure 4, D′ and D″, Movies available online) show the interaction of the microtubule with the cortex (arrows) and the subsequent furrow that forms in the polar region.

The above-mentioned data indicate that taxol-stabilized microtubules can initiate furrow formation where they contact the cortex. Even microtubules that emanate toward the poles, which are normally highly dynamic and are not associated with furrowing, can lead to furrow initiation when stabilized by taxol. Furthermore, it confirms previous data that overlapping microtubule plus ends are not required for furrow positioning (Canman *et al*., 2003).

Localization of Contractile Ring Components to Furrows Formed in Cells with Taxol-stabilized Microtubules

To test whether the furrows that formed at the ends of taxol-stabilized microtubules contained typical components, we examined their molecular composition. PtK1 cells ar-

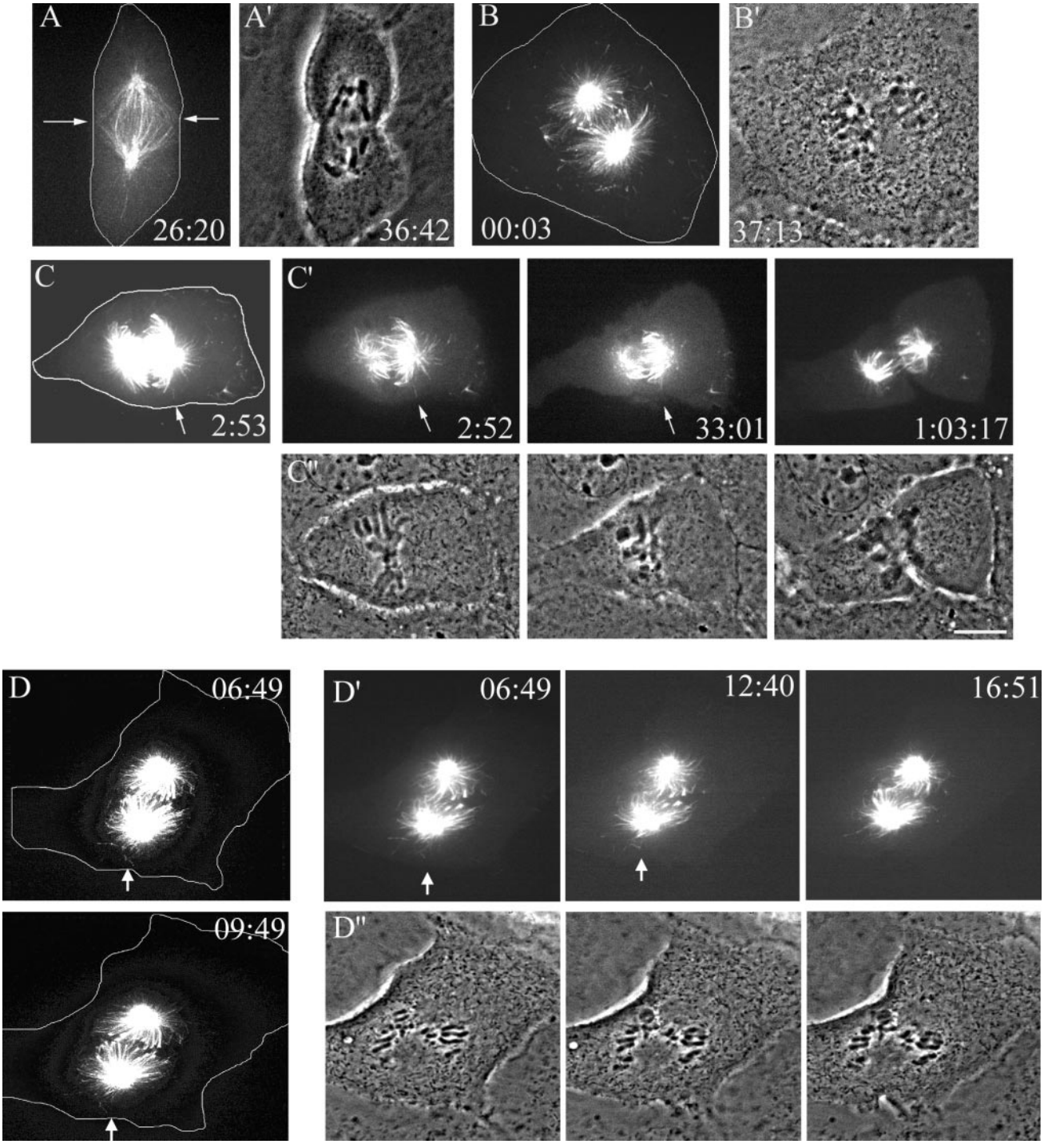

Figure 4. Taxol-stablized microtubules interact with the cortex at the site of eventual furrow formation. (A) Single plane projection of deconvolved optical sections of a control cell in early anaphase after injection with Mad2ΔC and rhodamine-tubulin. Arrows show position of microtubules at the cortex before furrowing. (A′) Phase contrast image of control cell 10 min later, showing the position of the furrow. (B) Single plane projection of deconvolved optical sections of a taxol-treated cell injected with Mad2ΔC and rhodamine-tubulin that did not form a furrow. Note the lack of microtubule contacts at the cortex. (B′) Phase contrast image of cell in B showing lack of furrow formation. (C) Single plane projection of deconvolved optical sections of a taxol-treated cell injected with Mad2ΔC and rhodamine-tubulin that formed a furrow. Arrow denotes microtubule interaction with the cortex. (C′) Single plane time lapse images showing microtubules. Arrows show the position of a microtubule interacting with the cortex. Note the lack of such contacts above the spindle. (C″) Single plane time-lapse phase contrast images show furrow progression and correspond to images in C′. (D) Two single plane projections of deconvolved optical sections of a taxol-treated cell injected with Mad2ΔC and rhodamine-tubulin that formed an abnormally positioned furrow. Arrow denotes microtubule interaction with the cortex. (D′) Single plane time-lapse images showing microtubules. Arrows show the position of a microtubule interacting with the cortex. (D″) Single plane time lapse phase contrast images show furrow progression and correspond to images in D′. Cell boundaries in A, B, C, and D were drawn using corresponding phase contrast images. Time is in hours:minutes:seconds, and for A, B, C and D are the time of the first image in the Z series. Contrast has been adjusted to highlight microtubule interactions with the cortex. Bar, 10 μm.

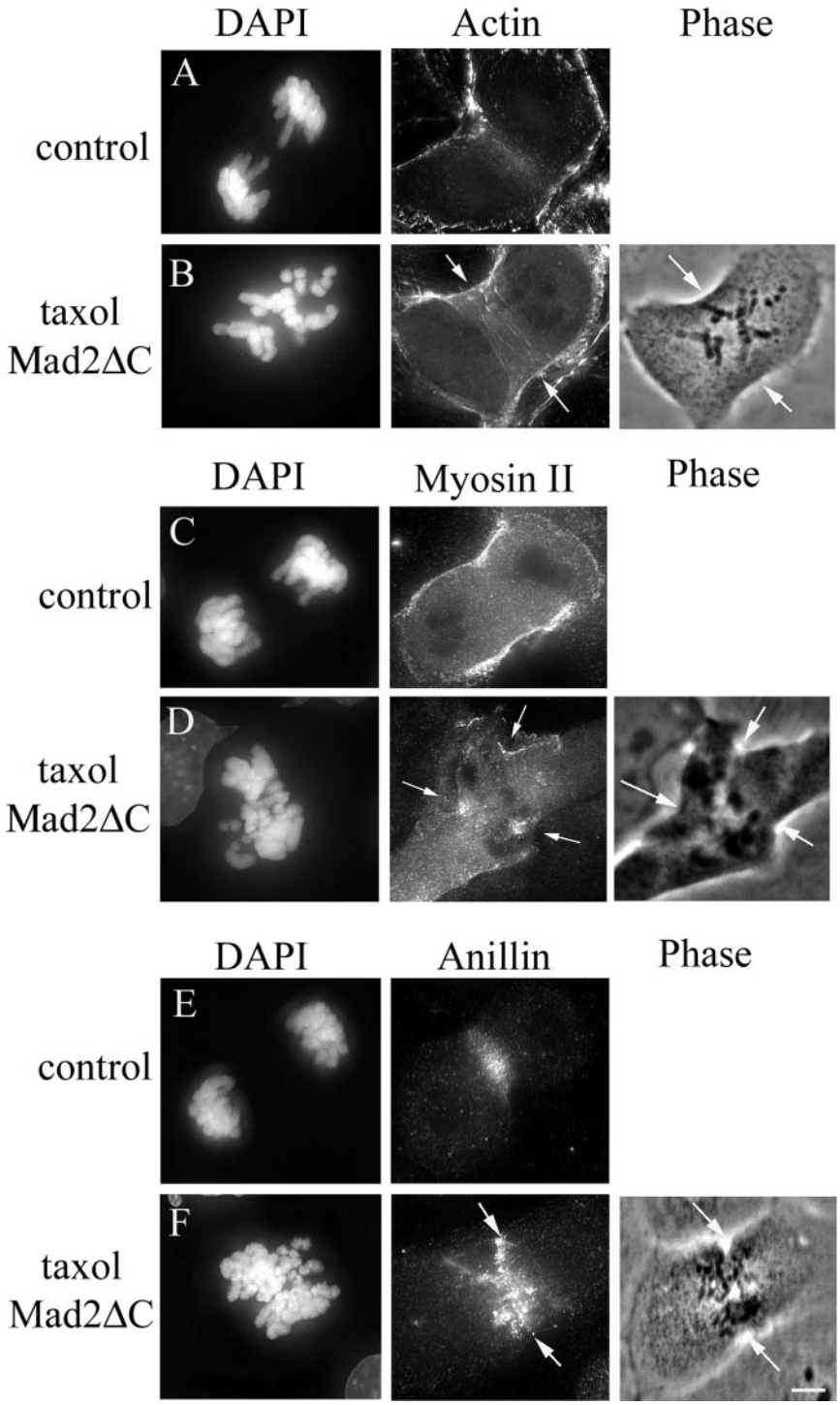

Figure 5. Immunolocalization of actin, myosin II, and anillin to the furrows formed in taxol-treated cells. All fluorescence images are single plane projections of deconvolved optical sections through the cell. Phase contrast images represent the last time point before fixation. (A) 4,6-Diamidino-2-phenylindole (DAPI) and phalloidin staining of control cell. Equatorial actin band looks faint because it is localized to the adherent cortex. (B) DAPI and phalloidin staining of taxol-treated, Mad2ΔC injected cell. Arrows mark site of furrowing. (C) DAPI staining and myosin II immunofluorescence in a control anaphase cell. (D) DAPI and myosin II staining of taxol-treated, Mad2ΔC-injected cell shows an accumulation of myosin II at the cortex in each of the three ingressions (arrows). (E) DAPI staining and anillin immunofluorescence in a control anaphase cell. (F) DAPI staining and anillin immunofluorescence in a taxol-treated, Mad2ΔC-injected cell. Anillin is localized to furrow region (arrows). Bar, 5 μm.

rested by taxol and injected with Mad2ΔC were followed by time-lapse phase microscopy and fixed shortly after furrow initiation. Anillin and INCENP, which normally localize to the cortex before furrow initiation as well as actin and myosin II localizations were examined.

Actin filaments in control PtK1 cells showed a similar organization to that seen in previous work (Sanger *et al.*, 1989; Fishkind and Wang, 1993). By phalloidin staining, actin was uniformly localized at the cortex through metaphase, with filaments often aligned along the spindle axis. In anaphase, actin filaments oriented perpendicular to the spindle axis concentrated at the adherent (ventral) surface of the cell after chromosome segregation to the poles. Figure 5A shows a single plane projection of deconvolved optical sections through an untreated control cell in anaphase, showing the separated chromosomes and actin at the furrow and in a band at the equator of the ventral cortex. In taxol-treated, Mad2ΔC injected cells that furrowed, phalloidin staining showed an accumulation of F-actin at the site of furrow ingression (n = 26) (Figure 5B). Myosin II distribution in

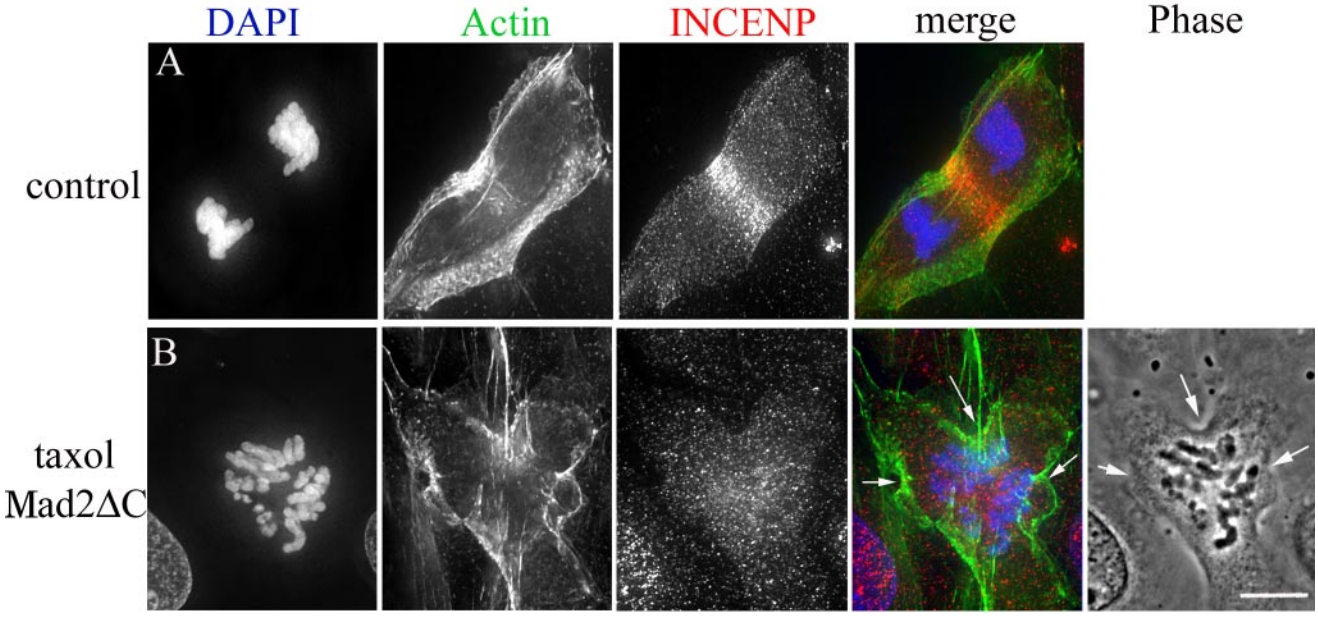

Figure 6. INCENP does not localize to furrows formed after microtubule stabilization by taxol. All fluorescence images are single plane projections of deconvolved optical sections through the cell. (A) 4,6-Diamidino-2-phenylindole (DAPI) and phalloidin staining and INCENP immunofluorescence in a control anaphase cell. (B) DAPI and phalloidin staining and INCENP immunofluorescence in a taxol-treated, Mad2 ΔC-injected cell. Notice the concentration of actin in the three ingressions (arrows). No INCENP is found at the cortex. Phase contrast image showing ingressions (arrows) is from last time point before fixation. Bar, 5 μm.

control cells, as visualized by immunofluorescence, was uniform along the cortex until late anaphase, when it became concentrated in and around the site of furrowing (Figure 5C). Twenty-one of 24 taxol-treated cells injected with Mad2ΔC showed enhanced myosin II localization at the ingressing furrow, as shown in Figure 5D. No actin or myosin II accumulation at the equator was seen in control or taxol-treated cells before anaphase.

We also examined the localization of anillin, a protein that interacts with actin and septins at the cortex in *Drosophilia* and human cells (Field and Alberts, 1995; Oegema *et al.*, 2000). Anillin became concentrated at the cytokinetic furrow in late anaphase in control PtK1 cells (Figure 5E). Anillin was localized to ingressing furrows in 16 of 18 PtK1 taxol-treated cells injected with Mad2ΔC. An example is shown in Figure 5F, where anillin is localized to the site of furrowing, although the band of anillin is not as well organized as in controls. The localization of anillin indicates that these furrows contain components of the contractile ring and are not random cortical contractions as seen in cells treated with nocodazole (Canman *et al.*, 2000). No anillin localization at the equatorial cortex was seen in untreated or taxol treated cells before anaphase onset. Our results are consistent with a study using the myosin II inhibitor blebbistatin, which reported that addition of taxol to anaphase cells treated with blebbistatin did not disrupt the localization of myosin II or anillin (Straight *et al.*, 2003).

We also determined the localization of INCENP, a chromosomal passenger protein that localizes to centromeres in mitosis and moves to the spindle midzone and equatorial cortex during anaphase, where it has been implicated in the completion of cytokinesis (Cooke *et al.*, 1987; Eckley *et al.*, 1997; Mackay *et al.*, 1998). In control PtK1 cells, INCENP localized to the equatorial cortex in anaphase between the separated chromosomes as expected (Figure 6A). In 14 taxol-treated cells that furrowed after injection of Mad2ΔC, we found no localization of INCENP at the cortex (Figure 6B). Whereas actin accumulated at the ingressions, INCENP showed diffuse localization near the chromosomes, indicating that it dissociated from the centromeres but did not localize to the cortex (Figure 6B). These data are consistent with a previous report that INCENP requires dynamic microtubules to localize to the cleavage furrow (Wheatley *et al.*, 2001) and provide further evidence that furrow initiation does not depend on INCENP localization to the cortex (Adams *et al.*, 2001).

Stabilization of Microtubules during Anaphase Affects the Timing of Furrow Initiation but Not Its Position

One possibility for the lack of furrowing, poor furrowing, and one-sided furrowing in some cells with stabilized preanaphase spindles is too few microtubule interactions with the cortex, because addition of taxol stabilized the short astral arrays typical of these spindles (Figure 4, B–D). Because astral microtubules grow rapidly during anaphase, we stabilized microtubules by adding taxol just after anaphase onset to try and increase the number of stable microtubules interacting with the cortex. To test the effects of microtubule stabilization during anaphase, we used PtK2 cells expressing GFP-α tubulin (Rusan *et al.*, 2001). Cells were followed by phase contrast microscopy, and taxol was added at the first sign of sister chromatid separation. In all cells treated with taxol after anaphase onset (n = 7), furrow position was normal, with ingressions on both sides of the spindle equator. However, there was a delay in the onset of furrow formation, with an average time of 22 ± 10 min from anaphase onset to furrow initiation, compared with 12 ± 4 min in control cells (n = 3). Unlike previous reports (Snyder and McLelland, 1996), there was no decrease in the rate of furrow progression, with an average time from furrow onset to maximum ingression of 13 ± 3 min in taxol-treated cells and 12 ± 3 min in controls.

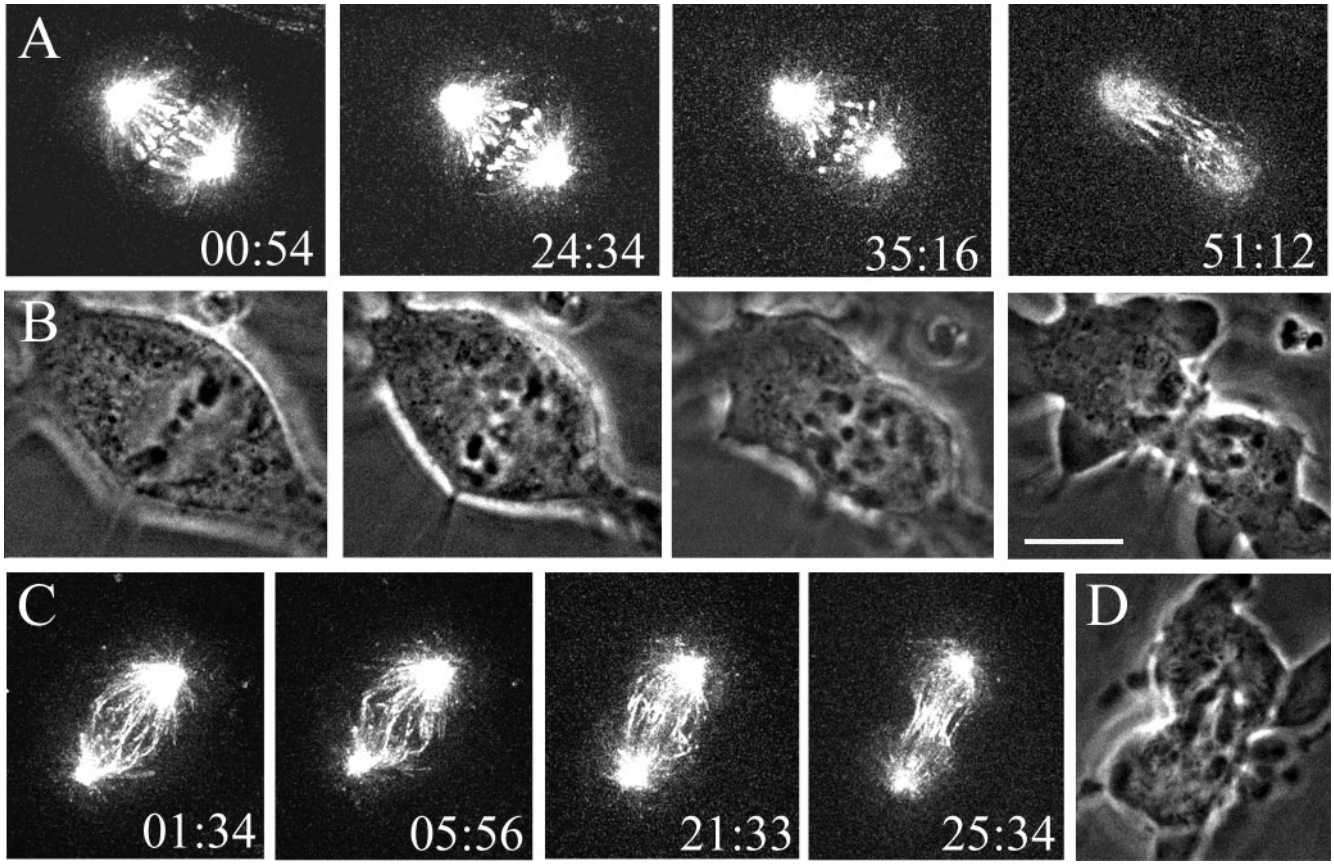

Figure 7. Stabilization of microtubules after anaphase onset does not affect furrow positioning. Taxol (10 μM) was added at T = 00:00. (A and C) Single plane projection of optical sections of GFP-tubulin images. Time is in minutes:seconds after taxol addition, and it is the time of the first image in the Z series. (B) Phase contrast images corresponding to images in A showing normal furrow positioning. (D) Phase contrast image corresponding to the last panel of C. Bar, 10 μm.

Deconvolution and single plane projection of GFP-tubulin images showed that these cells had numerous microtubules that interacted with the cortex at the position of the spindle equator. Two examples are shown in Figure 7. Note the increased number and length of astral microtubules compared with the spindles in Figure 4. Taxol was added very early in anaphase to the cell in Figure 7, A and B, and this cell furrowed normally even though it failed to form the central spindle, as evidenced by the lack of GFP-tubulin signal between the two half-spindles. The other six cells were similar to the one shown in Figure 7C, where anaphase A occurred before the addition of taxol, and cells were able to form a central spindle.

There was some blebbing in the polar regions of these cells (Figure 7, B and D), but because this blebbing also occurred in untreated GFP-α tubulin-expressing PtK2 cells, it cannot simply be due to a lack of dynamic microtubules. All cells treated with taxol after anaphase onset initiated furrows (7 of 7 initiate furrows), indicating more vigorous furrowing than cells treated with taxol in prometaphase or metaphase (9 of 12 initiate furrows). From these experiments, we conclude that taxol stabilization of anaphase spindle microtubules does not affect furrow position or rate of ingression, but it does cause a delay in the onset of furrowing.

Central Spindle Formation in the Presence of Taxol

The central spindle, or spindle midzone, forms during anaphase as interdigitating oppositely oriented microtubule plus ends are bundled by PRC1, which is essential for midzone formation (Mollinari *et al*., 2002). Previous studies indicated that this structure plays an important role in furrow induction in mammalian cells (Wheatley and Wang, 1996; Murata-Hori and Wang, 2002). However, monopolar cells undergo cytokinesis, although they lack a central spindle, and all microtubules are oriented in the same direction (Canman *et al*., 2003), casting doubt on the requirement of this structure for furrowing.

Our experiments visualizing microtubules in live cells suggested that there were differences in central spindle formation depending on when taxol was added. When taxol was added to cells with prometaphase or metaphase spindles and these cells were induced to enter anaphase by Mad2ΔC, the lack of microtubule dynamics prevented formation of the central spindle. Notice that the spindles in the cells in Figure 4 lack microtubule bundles between the half-spindles. However, six of seven cells treated with taxol after anaphase onset were able to form at least a partial central spindle (Figure 7).

We further examined midzone formation in our taxol-treated cells through tubulin and PRC1 immunofluorescence. In control anaphase cells, PRC1 was localized to the midzone as expected (Figure 8A; Jiang *et al*., 1998). In cells arrested by taxol in metaphase, PRC1 was diffusely localized on the spindle (Figure 8B). Cells that furrowed after treatment with 10 μM taxol at anaphase onset (n = 10) showed PRC1 localization to the plus ends of some, but not all

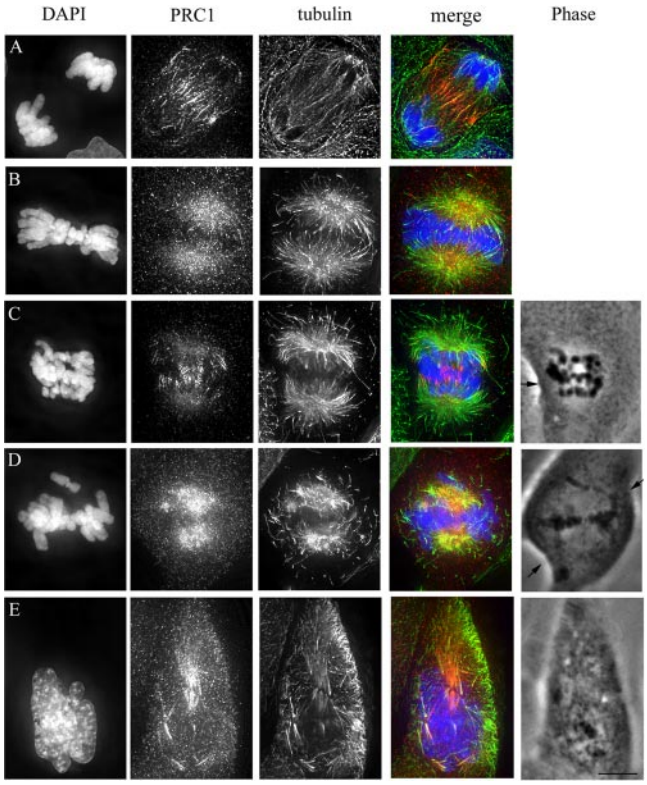

Figure 8. Analysis of midzone formation by tubulin and PRC1 immunofluorescence. All fluorescence images are single plane projections of deconvolved optical sections through the cell. (A) Untreated anaphase showing PRC1 localization to the midzone. (B) Taxol-arrested metaphase cell has diffuse PRC1 localization on the spindle. (C) Cell treated with taxol at anaphase onset. PRC1 has localized to the tips of microtubules. Phase contrast image shows furrow ingression (arrow) at the last time point before fixation. (D) Cell arrested with taxol and injected with Mad2ΔC to induce anaphase. PRC1 is concentrated on a subset of microtubules, even though the microtubules are not organized into interzonal bundles. Phase contrast image shows furrow ingression (arrows) at the last time point before fixation. (E) Cell arrested with taxol and injected with Mad2ΔC that did not furrow before exiting mitosis. Microtubule bundles with PRC1 localization persist. Phase contrast image shows the last time point before fixation. Bar, 10 μm.

microtubules, as well as PRC1 between the two half-spindles (Figure 8C). We did not observe tubulin immunofluorescence between the two half-spindles, but it is well known that epitope shielding occurs in this area of the spindle. Based on PRC1 localization and live cell imaging of GFP-α-tubulin cells (Figure 7), we conclude that cells treated with taxol after anaphase onset can form a central spindle. Cells induced to enter anaphase by Mad2ΔC injection after taxol treatment exhibited PRC1 on a few microtubules, regardless of whether or not furrowing occurred (n = 10) (Figure 7, D and E). However, unlike cells treated with taxol after anaphase onset, there was no PRC1 localized between the two half-spindles. Based on PRC1 localization and rhodamine tubulin imaging in live cells (Figure 4), we conclude that cells treated with taxol before anaphase onset do not form a central spindle. Our data do not rule out a role for PRC1 in furrow formation, but suggest that the presence of overlapping microtubule plus ends in the spindle midzone is not required for furrow initiation. These results confirm that the localization of PRC1 is cell-cycle regulated (Zhu and Jiang, 2005) and are consistent with recent findings that depletion of PRC1 in mammalian cells did not prevent furrow initiation or completion (Mollinari *et al*., 2005).

DISCUSSION

Taxol-stabilized Spindle Microtubules at the Cortex Correlate with Furrow Induction

Previously, analysis of microtubules during anaphase in PtK1 cells revealed a subset of stable microtubules that interacted with the equatorial cortex before furrow formation (Canman *et al*., 2003). This led to a model that these stable microtubules are responsible for positioning the cleavage plane. One prediction of the model, that stable microtubules position the cleavage furrow through contact with the cell cortex, is supported by our data. We observed a correlation between the location of stable microtubules and furrow position. We only observed furrowing in taxol-treated cells induced to enter anaphase where the plus end of a stable microtubule was proximal to the cortex. The position of these microtubules did not always correspond to the spindle equator, but for both normally and abnormally positioned furrows, a stable microtubule(s) contacted the cortex before furrow onset. The ability of polar astral microtubules, which are not normally associated with furrow formation, to induce furrowing after taxol stabilization where they contacted the polar cortex provides further evidence that stabilized microtubules can induce furrow formation. Cells that did not furrow lacked apparent microtubule contacts with the cortex. Whereas stabilized spindle microtubules were correlated with furrow formation, the short microtubules in the cytoplasm induced by taxol were not associated with furrowing (Figure 4). These findings suggest that stable spindle microtubules at the cortex positively regulate furrow formation.

In our current study, taxol-stabilized microtubules that contacted the cortex were able to elicit a furrowing response from the cortex, even though these microtubules were artificially stabilized. The structure of preassembled microtubules changes slightly after taxol is added (Arnal and Wade, 1995), so the taxol-stabilized microtubules in our experiments are likely to differ from the stable microtubules that are normally attached to the equatorial cortex at anaphase. We have shown that both types of stable microtubules lack concentrated EB1 at their plus ends, and both are associated with furrow initiation, even though they are stabilized by different mechanisms (Canman *et al*., 2003). In support of our data, recent experiments with taxol-treated sea urchin eggs show that the stabilized spindle can cause furrowing if brought into contact with the cortex (David Burgess, personal communication). We conclude that nondynamic plus ends of spindle microtubules are able to induce furrowing when they persist in contacting the cortex.

How can we reconcile our model for positioning of the cleavage furrow by stable microtubules with the ectopic Rappaport furrows that form between spindle poles lacking intervening chromosomes? Stable microtubules were not previously observed in the polar regions of dividing PtK1 cells (Canman *et al*., 2003); however, it is possible that astral microtubules from two independent spindles may become stabilized due to interdigitating plus ends or cross-linking of oppositely oriented microtubules by microtubule-associated proteins. Rappaport furrows in PtK1 cells have previously been associated with the presence of overlapping microtubules (Savoian *et al*., 1999). However, it remains to be shown whether these microtubules were stabilized or in contact with cortex.

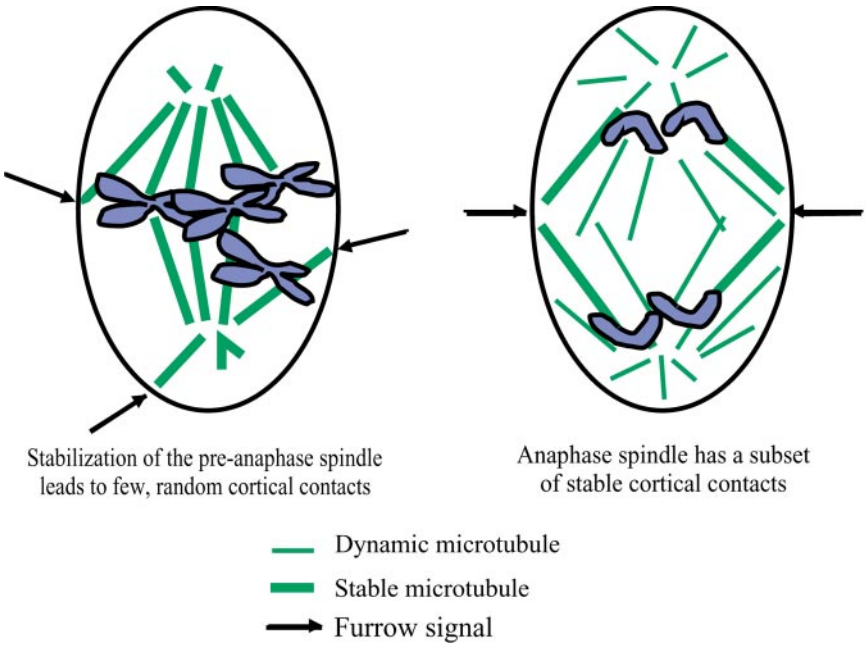

Figure 9. Model for induction of furrow positioning after microtubule stabilization in metaphase versus anaphase. Left cell illustrates that stabilization of microtubules before anaphase onset leads to few, random contacts with the cortex. At anaphase onset, this results in abnormal furrow positioning. Right cell shows that normally during anaphase a subset of microtubules are relatively stable, leading to induction of the furrow at the equator.

Our data also show that the central spindle is not required for furrow initiation in mammalian cells. PtK1 cells treated with taxol before anaphase onset can furrow, even though overlapping microtubule bundles between segregated chromosomes are not able to form. This extends previous findings that overlapping microtubules are not required for furrow formation (Canman *et al*., 2003).

Why Does Stabilization of Preanaphase Spindles Result in Abnormal Furrow Positioning and Lack of Furrowing in Some Cells?

Several lines of evidence suggest that the entire cell cortex becomes capable of responding to the cleavage signal between anaphase onset and exit from mitosis. In mammalian cells, inducing anaphase onset in the absence of microtubules leads to global cortical contractions, and furrows can form if microtubules are allowed to repolymerize during a window of about an hour, a period termed C phase (Canman *et al*., 2000). In an echinoderm egg, repositioning of the mitotic apparatus during this period can lead to the formation of up to 13 different furrows (Rappaport, 1985). Both these studies indicate that multiple regions of the cortex are capable of responding to the cleavage signal. This is consistent with our data that any region of the cortex, independent of spindle orientation, is capable of furrowing in anaphase if contacted by a stable microtubule.

We suspect that one explanation for the lack of furrowing and abnormal furrow positioning in cells treated with taxol before anaphase onset is due to the stabilization of the short microtubule arrays typical of the preanaphase spindle. Anaphase spindles have longer astral microtubules and greater numbers of microtubules interacting with the cortex than metaphase spindles (compare Figure 4, A and C). Even though Mad2ΔC induces anaphase by activating the APC/C (Luo *et al*., 2000; Canman *et al*., 2002), the presence of taxol prevents the rearrangement of microtubules that usually accompanies anaphase onset. As a result, the microtubule contacts with the cortex are few and random, which could account for the variability in the presence and position of furrows in these cells (Figure 9). We saw a correlation between cell size and furrowing, with smaller cells more likely to form a furrow. If stabilized microtubules can induce a furrow only when they contact the cortex, then cells of larger area would be less likely to contain these random contacts. Therefore, stabilization of the preanaphase spindle sometimes results in a lack of microtubule–cortex interactions and a failure to furrow, especially in larger cells. In support of this idea, we found that stabilizing the long microtubules that grew immediately after anaphase onset produced numerous microtubule-cortex interactions, particularly at the equator. This stabilization resulted in correct furrow placement (Figures 7 and 9). Therefore, the growth of numerous microtubules to the cortex during early anaphase is likely required to provide a strong stimulus for proper furrowing (Figure 9).

What is the Role of Dynamic Microtubules in Cytokinesis?

Our studies indicate that the strength of the stimulus for furrowing depends on the location and number of stabile microtubule ends proximal to the cortex. It is not surprising that a single or few microtubule ends contacting the cortex would result in a delay in furrow formation compared with the normal timing with a large anaphase array. However, it was unexpected to see the 10-min delay that resulted when cells entering anaphase were treated with taxol. Long, stable microtubules were formed in these cells that extended out to the equatorial cortex. Once furrowing began, ingression progressed at normal velocities.

These data indicate that dynamic microtubules are not strictly required for furrow positioning or a normal rate of furrow ingression but that they do accelerate the timing of furrow formation. If reduction in the number of microtubule-cortical contacts is not the cause of the delay, other possibilities include loss of contributions from growing ends or from an incomplete midzone microtubule complex. Microtubule polymerization may recruit a plus end tracking protein or an unknown factor which could play a role in accelerating furrow formation at the equator. Dynamic microtubules could also contribute to timely furrowing by

promoting relaxation at polar cortical regions, allowing contraction at the equator to occur more rapidly. Further experimentation will be needed to distinguish between these possibilities.

Whereas furrow positioning and initiation were able to occur in the presence of taxol, cells were not able to complete cytokinesis. Therefore, microtubule dynamics are required for furrow completion. A simple explanation may be that the stabilization of microtubules by taxol may have created a physical block to complete furrow ingression. Another possibility is that because dynamic microtubules are required for localization of INCENP (Wheatley *et al*., 2001), furrows regressed due to lack of INCENP at the cortex. Alternatively, microtubules may play a more direct role in furrow completion. Because midzone microtubules are required for furrow completion (Wheatley and Wang, 1996), and taxol prevents normal central spindle formation when added before anaphase onset (Figure 8) (Amin-Hanjani and Wadsworth, 1991; Snyder and McLelland, 1996), blocking microtubule dynamics may inhibit furrow completion due to the lack of a midzone. Interestingly, furrows formed in cells lacking a midzone (those treated with taxol before anaphase) often regressed, whereas furrows formed in cells with a midzone (treated with taxol after anaphase onset) progressed farther and did not regress.

Nature of Stimulatory Signal

What is it about stable microtubules that elicit a furrowing response from the cortex? It may be that the stable microtubule plus ends directly induce contractility. One possible mechanism would be the regulation of a GTPase by stable microtubule ends (Canman *et al*., 2003). It has been shown in mammalian cells that the growth of microtubules activates the Rac1 GTPase, leading to actin polymerization in the leading edge of lamellipodia (Waterman-Storer *et al*., 1999; Canman *et al*., 2003). GTPases of the Rho family have been shown to be important for cytokinesis in a number of systems (Kishi *et al*., 1993; Mabuchi *et al*., 1993; O'Connell *et al*., 1999; Tolliday *et al*., 2002). Perhaps the presence of stable microtubules at the cortex locally activates Rho GTPases, leading to furrow formation. Alternatively, stable microtubules could promote delivery of a stimulating factor along microtubules to the cell cortex or removal of an inhibitory factor from a specific cortical region. By this mechanism, stable attachment of the microtubule plus end to the cortex would concentrate at this site a stimulatory factor transported along the microtubules. This would suggest an important role for kinesins, which could transport the stimulating molecule toward plus ends to the cortex or directly act to induce furrow formation. There is evidence that the kinesin PAV-KLP/ZEN-4/Chinese hamster ovary-1 is involved in cytokinesis, although whether it is required for furrow initiation or completion is unclear (Adams *et al*., 1998; Kuriyama *et al*., 2002; Matuliene and Kuriyama, 2002). Although it has long been appreciated that microtubules are required for furrow positioning, the molecular nature of the signal has yet to be elucidated.

ACKNOWLEDGMENTS

We thank Pat Wadsworth (University of Massachusetts, Amherst, MA) for GFP-α tubulin-expressing cells, Aaron Straight (Stanford University School of Medicine, Stanford, CA) and Christine Field (Harvard Medical School, Boston, MA) for antibodies, and Lisa Cameron for labeled tubulin. K.B.S. is a fellow in the Seeding Postdoctoral Innovators in Science and Education (SPIRE) program supported by the Minority Opportunities in Research Division of National Institute of General Medical Sciences Grant GM-000678. E.D.S. is supported by National Institutes of Health Grant GM-24364.

REFERENCES

Adams, R. R., Maiato, H., Earnshaw, W. C., and Carmena, M. (2001). Essential roles of Drosophila inner centromere protein (INCENP) and aurora B. in histone H3 phosphorylation, metaphase chromosome alignment, kinetochore disjunction, and chromosome segregation. J. Cell Biol. *153*, 865–880.

Adams, R. ., Tavares, A. A., Salzberg, A., Bellen, H. J., and Glover, D. M. (1998). pavarotti encodes a kinesin-like protein required to organize the central spindle and contractile ring for cytokinesis. Genes Dev. *12*, 1483–1494.

Alsop, G. B., and Zhang, D. (2003). Microtubules are the only structural constituent of the spindle apparatus required for induction of cell cleavage. J. Cell Biol. *162*, 383–390.

Amin-Hanjani, S., and Wadsworth, P. (1991). Inhibition of spindle elongation by taxol. Cell Motil. Cytoskeleton *20*, 136–144.

Amos, L. A., and Lowe, J. (1999). How Taxol stabilises microtubule structure. Chem. Biol. *6*, R65–R69.

Arnal, I., and Wade, R. H. (1995). How does taxol stabilize microtubules? Curr. Biol. *5*, 900–908.

Beams, H. W., and Evans, T. C. (1940). Some effects of colchicine upon the first cleavage in *Arbacia punctulata*. The Biol. Bull. *79*, 188–198.

Canman, J. C., Cameron, L. A., Maddox, P. S., Straight, A., Tirnauer, J. S., Mitchison, T. J., Fang, G., Kapoor, T. M., and Salmon, E. D. (2003). Determining the position of the cell division plane. Nature *424*, 1074–1078.

Canman, J. C., Hoffman, D. B., and Salmon, E. D. (2000). The role of pre- and post-anaphase microtubules in the cytokinesis phase of the cell cycle. Curr. Biol. *10*, 611–614.

Canman, J. C., Salmon, E. D., and Fang, G. (2002). Inducing precocious anaphase in cultured mammalian cells. Cell Motil. Cytoskeleton *52*, 61–65.

Cao, L. G., and Wang, Y. L. (1996). Signals from the spindle midzone are required for the stimulation of cytokinesis in cultured epithelial cells. Mol. Biol. Cell *7*, 225–232.

Conklin, E. G. (1917). Effects of centrifugal force on the structure and development of the eggs of *Crepidula*. J. Exp. Zool. *22*, 311–419.

Cooke, C. A., Heck, M. M., and Earnshaw, W. C. (1987). The inner centromere protein (INCENP) antigens: movement from inner centromere to midbody during mitosis. J. Cell Biol. *105*, 2053–2067.

De Brabander, M., Geuens, G., Nuydens, R., Willebrords, R., Aerts, F., and De Mey, J. (1986). Microtubule dynamics during the cell cycle: the effects of taxol and nocodazole on the microtubule system of Pt K2 cells at different stages of the mitotic cycle. Int. Rev. Cytol. *101*, 215–274.

De Brabander, M., Geuens, G., Nuydens, R., Willebrords, R., and De Mey, J. (1981). Taxol induces the assembly of free microtubules in living cells and blocks the organizing capacity of the centrosomes and kinetochores. Proc. Natl. Acad. Sci. USA *78*, 5608–5612.

Dechant, R., and Glotzer, M. (2003). Centrosome separation and central spindle assembly act in redundant pathways that regulate microtubule density and trigger cleavage furrow formation. Dev. Cell *4*, 333–344.

Eckley, D. M., Ainsztein, A. M., Mackay, A. M., Goldberg, I. G., and Earnshaw, W. C. (1997). Chromosomal proteins and cytokinesis: patterns of cleavage furrow formation and inner centromere protein positioning in mitotic heterokaryons and mid-anaphase cells. J. Cell Biol. *136*, 1169–1183.

Field, C. M., and Alberts, B. M. (1995). Anillin, a contractile ring protein that cycles from the nucleus to the cell cortex. J. Cell Biol. *131*, 165–178.

Fishkind, D. J., and Wang, Y. L. (1993). Orientation and three-dimensional organization of actin filaments in dividing cultured cells. J. Cell Biol. *123*, 837–848.

Hamaguchi, Y. (1975). Microinjection of colchicine into sea urchin eggs. Dev Growth Differ *17*, 111–117.

Hamaguchi, Y. (1998). Displacement of cleavage plane in the sea urchin egg by locally applied taxol. Cell Motil. Cytoskeleton *40*, 211–219.

Harvey, E. B. (1935). The mitotic figure and cleavage plane in the egg of *Parechinus microtuberculatus*, as influenced by centrifugal force. Biol. Bull. *69*, 287–297.

Hiramoto, Y. (1956). Cell division without mitotic apparatus in sea urchin eggs. Exp. Cell Res. *11*, 630–636.

Hyman, A., Drechsel, D., Kellogg, D., Salser, S., Sawin, K., Steffen, P., Wordeman, L., and Mitchison, T. (1991). Preparation of modified tubulins. Methods Enzymol *196*, 478–485.

Jiang, W., Jimenez, G., Wells, N. J., Hope, T. J., Wahl, G. M., Hunter, T., and Fukunaga, R. (1998). PRC 1, a human mitotic spindle-associated CDK substrate protein required for cytokinesis. Mol Cell *2*, 877–885.

Kishi, K., Sasaki, T., Kuroda, S., Itoh, T., and Takai, Y. (1993). Regulation of cytoplasmic division of Xenopus embryo by rho p21 and its inhibitory GDP/GTP exchange protein (rho GDI). J. Cell Biol. *120*, 1187–1195.

Kuriyama, R., Gustus, C., Terada, Y., Uetake, Y., and Matuliene, J. (2002). CHO1, a mammalian kinesin-like protein, interacts with F-actin and is involved in the terminal phase of cytokinesis. J. Cell Biol. *156*, 783–790.

Luo, X., Fang, G., Coldiron, M., Lin, Y., Yu, H., Kirschner, M. W., and Wagner, G. (2000). Structure of the Mad2 spindle assembly checkpoint protein and its interaction with Cdc20. Nat. Struct. Biol. *7*, 224–229.

Mabuchi, I., Hamaguchi, Y., Fujimoto, H., Morii, N., Mishima, M., and Narumiya, S. (1993). A rho-like protein is involved in the organisation of the contractile ring in dividing sand dollar eggs. Zygote *1*, 325–331.

Mabuchi, I., and Okuno, M. (1977). The effect of myosin antibody on the division of starfish blastomeres. J. Cell Biol. *74*, 251–263.

Mackay, A. M., Ainsztein, A. M., Eckley, D. M., and Earnshaw, W. C. (1998). A dominant mutant of inner centromere protein (INCENP), a chromosomal protein, disrupts prometaphase congression and cytokinesis. J. Cell Biol. *140*, 991–1002.

Maddox, P. S., Moree, B., Canman, J. C., and Salmon, E. D. (2003). Spinning disk confocal microscope system for rapid high-resolution, multimode, fluorescence speckle microscopy and green fluorescent protein imaging in living cells. Methods Enzymol. *360*, 597–617.

Martineau, S. N., Andreassen, P. R., and Margolis, R. L. (1995). Delay of HeLa cell cleavage into interphase using dihydrocytochalasin B: retention of a postmitotic spindle and telophase disc correlates with synchronous cleavage recovery. J. Cell Biol. *131*, 191–205.

Matuliene, J., and Kuriyama, R. (2002). Kinesin-like protein CHO1 is required for the formation of midbody matrix and the completion of cytokinesis in mammalian cells. Mol. Biol. Cell *13*, 1832–1845.

Mollinari, C., Kleman, J. P., Jiang, W., Schoehn, G., Hunter, T., and Margolis, R. L. (2002). PRC1 is a microtubule binding and bundling protein essential to maintain the mitotic spindle midzone. J. Cell Biol. *157*, 1175–1186.

Mollinari, C., Kleman, J. P., Saoudi, Y., Jablonski, S. A., Perard, J., Yen, T. J., and Margolis, R. L. (2005). Ablation of PRC1 by small interfering RNA demonstrates that cytokinetic abscission requires a central spindle bundle in mammalian cells, whereas completion of furrowing does not. Mol. Biol. Cell *16*, 1043–1055.

Morrison, E. E., Wardleworth, B. N., Askham, J. M., Markham, A. F., and Meredith, D. M. (1998). EB1, a protein which interacts with the APC tumour suppressor, is associated with the microtubule cytoskeleton throughout the cell cycle. Oncogene *17*, 3471–3477.

Murata-Hori, M., and Wang, Y. L. (2002). Both midzone and astral microtubules are involved in the delivery of cytokinesis signals: insights from the mobility of aurora B. J. Cell Biol. *159*, 45–53.

O'Connell, C. B., Wheatley, S. P., Ahmed, S., and Wang, Y. L. (1999). The small GTP-binding protein rho regulates cortical activities in cultured cells during division. J. Cell Biol. *144*, 305–313.

Oegema, K., Savoian, M. S., Mitchison, T. J., and Field, C. M. (2000). Functional analysis of a human homologue of the Drosophila actin binding protein anillin suggests a role in cytokinesis. J. Cell Biol. *150*, 539–552.

Rappaport, R. (1985). Repeated furrow formation from a single mitotic apparatus in cylindrical sand dollar eggs. J. Exp. Zool. *234*, 167–171.

Rappaport, R. (1986). Establishment of the mechanism of cytokinesis in animal cells. Int. Rev. Cytol. *105*, 245–281.

Rappaport, R., and Ebstein, R. P. (1965). Duration of stimulus and latent periods preceding furrow formation in sand dollar eggs. J. Exp. Zool. *158*, 373–382.

Rappaport, R., and Rappaport, B. N. (1974). Establishment of cleavage furrows by the mitotic spindle. J. Exp. Zool. *189*, 189–196.

Rieder, C. L., and Hard, R. (1990). Newt lung epithelial cells: cultivation, use, and advantages for biomedical research. Int. Rev. Cytol. *122*, 153–220.

Rusan, N. M., Fagerstrom, C. J., Yvon, A. M., and Wadsworth, P. (2001). Cell cycle-dependent changes in microtubule dynamics in living cells expressing green fluorescent protein-alpha tubulin. Mol. Biol. Cell *12*, 971–980.

Salmon, E. D., and Wolniak, S. M. (1984). Taxol stabilization of mitotic spindle microtubules: analysis using calcium-induced depolymerization. Cell Motil. *4*, 155–167.

Salmon, E. D., and Wolniak, S. M. (1990). Role of microtubules in stimulating cytokinesis in animal cells. Ann. N.Y. Acad. Sci. *582*, 88–98.

Sanger, J. M., Mittal, B., Dome, J. S., and Sanger, J. W. (1989). Analysis of cell division using fluorescently labeled actin and myosin in living PtK2 cells. Cell Motil. Cytoskeleton *14*, 201–219.

Savoian, M. S., Earnshaw, W. C., Khodjakov, A., and Rieder, C. L. (1999). Cleavage furrows formed between centrosomes lacking an intervening spindle and chromosomes contain microtubule bundles, INCENP, and CHO1 but not CENP-E. Mol. Biol. Cell *10*, 297–311.

Schiff, P. B., Fant, J., and Horwitz, S. B. (1979). Promotion of microtubule assembly in vitro by taxol. Nature *277*, 665–667.

Schiff, P. B., and Horwitz, S. B. (1980). Taxol stabilizes microtubules in mouse fibroblast cells. Proc. Natl. Acad. Sci. USA *77*, 1561–1565.

Schroeder, T. E. (1972). The contractile ring. II. Determining its brief existence, volumetric changes, and vital role in cleaving *Arbacia* eggs. J. Cell Biol. *53*, 419–434.

Shannon, K. B., Canman, J. C., and Salmon, E. D. (2002). Mad2 and BubR1 function in a single checkpoint pathway that responds to a loss of tension. Mol. Biol. Cell *13*, 3706–3719.

Snyder, J. A., and McLelland, S. L. (1996). Taxol reduces the rate of cytokinesis in PtK1 cells. Cell Biol. Int. *20*, 573–578.

Snyder, J. A., and Mullins, J. M. (1993). Analysis of spindle microtubule organization in untreated and taxol-treated PtK1 cells. Cell Biol. Int. *17*, 1075–1084.

Straight, A. F., Cheung, A., Limouze, J., Chen, I., Westwood, N. J., Sellers, J. R., and Mitchison, T. J. (2003). Dissecting temporal and spatial control of cytokinesis with a myosin II Inhibitor. Science *299*, 1743–1747.

Tirnauer, J. S., Canman, J. C., Salmon, E. D., and Mitchison, T. J. (2002). EB1 targets to kinetochores with attached, polymerizing microtubules. Mol. Biol. Cell *13*, 4308–4316.

Tolliday, N., VerPlank, L., and Li, R. (2002). Rho1 directs formin-mediated actin ring assembly during budding yeast cytokinesis. Curr. Biol. *12*, 1864–1870.

Waterman-Storer, C. M., Desai, A., Bulinski, J. C., and Salmon, E. D. (1998). Fluorescent speckle microscopy, a method to visualize the dynamics of protein assemblies in living cells. Curr. Biol. *8*, 1227–1230.

Waterman-Storer, C. M., Worthylake, R. A., Liu, B. P., Burridge, K., and Salmon, E. D. (1999). Microtubule growth activates Rac1 to promote lamellipodial protrusion in fibroblasts. Nat. Cell Biol. *1*, 45–50.

Waters, J. C., Mitchison, T. J., Rieder, C. L., and Salmon, E. D. (1996). The kinetochore microtubule minus-end disassembly associated with poleward flux produces a force that can do work. Mol. Biol. Cell *7*, 1547–1558.

Wheatley, S. P., Kandels-Lewis, S. E., Adams, R. R., Ainsztein, A. M., and Earnshaw, W. C. (2001). INCENP binds directly to tubulin and requires dynamic microtubules to target to the cleavage furrow. Exp. Cell Res. *262*, 122–127.

Wheatley, S. P., and Wang, Y. (1996). Midzone microtubule bundles are continuously required for cytokinesis in cultured epithelial cells. J. Cell Biol. *135*, 981–989.

Yvon, A. M., Wadsworth, P., and Jordan, M. A. (1999). Taxol suppresses dynamics of individual microtubules in living human tumor cells. Mol. Biol. Cell *10*, 947–959.

Zhu, C., and Jiang, W. (2005). Cell cycle-dependent translocation of PRC1 on the spindle by Kif4 is essential for midzone formation and cytokinesis. Proc. Natl. Acad. Sci. USA *102*, 343–348.